Structural Comparison of Anticancer Drug–DNA Complexes: Adriamycin and Daunomycin†,‡

Christine A. Frederick,§ Loren Dean Williams,§ Giovanni Ughetto,∥ Gijs A. van der Marel,⊥ Jacques H. van Boom,⊥ Alexander Rich,§ and Andrew H.-J. Wang*,§,#

Department of Biology, Massachusetts Institute of Technology, Cambridge, Massachusetts 02139, Instituto di Strutturistica Chimica, CNR, Area della Ricerca di Roma-Montelibretti, Rome, Italy, and Gorlaeus Laboratories, Leiden State University, 2300RA Leiden, The Netherlands

Received April 3, 1989; Revised Manuscript Received August 14, 1989

ABSTRACT: The anticancer drugs adriamycin and daunomycin have each been crystallized with the DNA sequence d(CGATCG) and the three-dimensional structures of the complexes solved at 1.7- and 1.5-Å resolution, respectively. These antitumor drugs have significantly different clinical properties, yet they differ chemically by only the additional hydroxyl at C14 of adriamycin. In these complexes the chromophore is intercalated at the CpG steps at either end of the DNA helix with the amino sugar extended into the minor groove. Solution of the structure of daunomycin bound to d(CGATCG) has made it possible to compare it with the previously reported structure of daunomycin bound to d(CGTACG). Although the two daunomycin complexes are similar, there is an interesting sequence dependence of the binding of the amino sugar to the A–T base pair outside the intercalation site. The complex of daunomycin with d(CGATCG) has tighter binding than the complex with d(CGTACG), leading us to infer a sequence preference in the binding of this anthracycline drug. The structures of daunomycin and adriamycin with d(CGATCG) are very similar. However, there are additional solvent interactions with the adriamycin C14 hydroxyl linking it to the DNA. Surprisingly, under the influence of the altered solvation, there is considerable difference in the conformation of spermine in these two complexes. The observed changes in the overall structures of the ternary complexes amplify the small chemical differences between these two antibiotics and provide a possible explanation for the significantly different clinical activities of these important drugs.

The daunomycin family of anthracycline antibiotics are effective in treating a variety of cancers. A large number of natural and synthetic analogues, consisting of an aromatic aglycon chromophore and an amino sugar (Figure 1), have been tested for biological activity (Arcamone, 1978, 1981; Brown, 1983). Chemical substituents on the fused ring system and on the amino sugar attenuate the therapeutic properties of the various members of this family of drugs. Slight changes in chemical structure cause significant changes in clinical properties. For example, daunomycin is most effective in treatment of leukemias, while the closely related adriamycin (14-hydroxyldaunomycin) is more effective in the treatment of solid tumors (DiMarco et al., 1974; Arcamone, 1981).

A variety of biochemical evidence suggests that the anthracyclines function primarily at the DNA level by blocking the processes of replication and transcription (Zunino et al., 1974). Although their interactions with other cellular targets may play a role in the selective cytotoxicity of these drugs, it is the binding to DNA that is generally believed to be essential for their activity. Due to the wide range of derivatives available and their importance in cancer chemotherapy, many attempts have been made to understand the key features responsible for the biological activity of this family of antibiotics (Arcamone, 1984), particularly the interactions with chromosomal DNA (Zunino et al., 1980; Grimmond & Beerman, 1982). Daunomycin binds to DNA with some preference for alternating pyrimidine–purine tracts as seen by thermal stabilization and fluorescence quenching techniques (DuVernay et al., 1979; Phillips et al., 1978). Changes in physical properties of both DNA and drug upon binding were consistent with intercalation of the chromophore, preferentially at CpG steps (Plumbridge & Brown, 1977; Chaires, 1983).

The first X-ray diffraction studies of oriented fibers of a daunomycin–DNA complex suggested a conformation similar to that of B-DNA with the chromophore inserted between base pairs (Pigram et al., 1972). The detailed interactions between daunomycin and DNA were later revealed by the single-crystal X-ray solution of the three-dimensional structure of a daunomycin–DNA complex (Quigley et al., 1980; Wang et al., 1987). Two daunomycin molecules bind to each DNA duplex of sequence d(CGTACG) to form a complex, referred to here as daun–TA. In daun–TA, the three ring planar chromophore of daunomycin is intercalated at the CpG steps on either end of the DNA helix. The amino sugar lies in the minor groove, forming hydrogen bonds to solvent water molecules. This structure suggested specific ways in which the biological function could be related to the structure. The orientation of the intercalated ring system, rings B, C, and D (see Figure 1), relative to the DNA helix might be changed by addition or removal of substituents of the fused ring system. Also, substitutions on the nonplanar ring (ring A) that alter its conformation could change the position of the amino sugar in the minor groove. In addition, the sequence-dependent conformation dictated by the DNA base pairs adjacent to the intercalation site may introduce other specificity requirements for the amino sugar moiety. Finally, the presence of different substituent groups may also affect the activity of the drug via their interaction with solvent molecules, ions, or other larger

† The research was supported by grants from the National Institutes of Health, the American Cancer Society, the National Science Foundation, and the Office of Naval Research.

‡ The atomic coordinates in this paper have been submitted to the Protein Data Bank.

* To whom correspondence should be addressed.

§ Massachusetts Institute of Technology.

∥ Instituto di Strutturistica Chimica, CNR.

⊥ Leiden State University.

Present address: Department of Physiology and Biophysics, University of Illinois at Urbana–Champaign, Urbana, IL 61801.

0006-2960/90/0429-2538$02.50/0

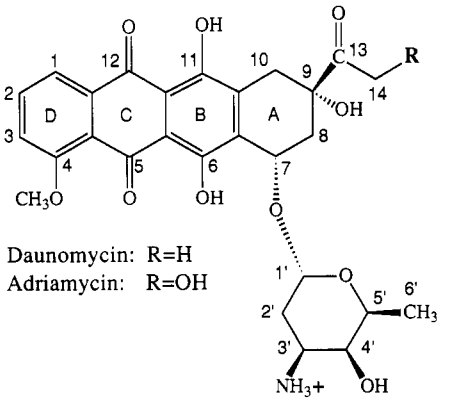

FIGURE 1: Schematic representation of adriamycin and daunomycin. The different functional groups are indicated.

ligands such as polyamines or proteins.

To help understand the relationship between anthracycline structure and function, we have solved the structure of additional complexes of varying drug substitution and DNA sequence. One complex described here is formed by a second important anthracycline derivative, adriamycin, bound to d(CGATCG). This complex is referred to here as adri–AT. This member of the anthracycline family has the widest spectrum of antitumor activity and is formed simply by the addition of a hydroxyl group to the 14-position of daunomycin. A second complex described here is formed by daunomycin bound to the same sequence, d(CGATCG). This complex is referred to here as daun–AT. In comparison with the previously reported daun–TA, the central A–T base pairs have been switched in adri–AT and daun–AT, while the CpG intercalation site has been preserved. Comparison of these three analogous complexes may allow us to understand on the molecular level how the chemical structures of the anthracyclines determine their biological function. Structural comparison of adriamycin and daunomycin both bound to the same sequence, d(CGATCG), reveals the involvement of the adriamycin C14-hydroxyl group in solvent interactions, as well as an unexpected modification of the manner in which a spermine molecule binds to these otherwise similar complexes. Further, structural comparison of daunomycin bound to d(CGTACG) or d(CGATCG) reveals an interesting change in the position of the charged amino group of the sugar moiety of the drug in the minor groove. The hydrogen bonding and van der Waal contacts are modified in the two structures, leading us to infer sequence-dependent alterations in binding constants. A preliminary report of this comparison has been presented (Frederick et al., 1985) and the comparison described briefly elsewhere (Ughetto, 1988).

Experimental Procedures

The self-complementary DNA hexamer was synthesized by the phosphotriester method (van der Marel et al., 1981) and purified by Sephadex G-50 chromatography. The final product was judged to be greater than 95% pure by HPLC. Adriamycin was kindly supplied by Farmitalia Carlo Erba, Milan, Italy. Both crystals were grown at room temperature in sitting drops by using the vapor diffusion technique. The crystallization mother liquor contained 2 mM DNA (single-strand concentration), 20 mM sodium cacodylate buffer, pH 6.5, 15 mM $MgCl_2$, 10 mM spermine, and 5% 2,4-methylpentanediol (MPD). The drops were equilibrated against a reservoir of 30% MPD. The drugs were included in the crystallization mixture in varying molar ratios to the DNA. The best crystals grew from a solution containing drug to duplex DNA in a ratio of 2:1. Tetragonal crystals began to appear within 2 weeks and grew to a size of about 0.3 mm × 0.3 mm × 0.15 mm. Unit cell determinations showed that they both crystallized in space group $P4_12_12$ with dimensions similar not only to each other but to the daun–TA complex as well. The lattice constants are $a = b = 28.21$ Å and $c = 53.19$ Å, or $a = b = 28.11$ Å and $c = 53.08$ Å, for the adria–AT and daun–AT complexes, respectively.

Data were collected on a Nicolet P3 diffractometer at 15 °C using an ω scan mode. In each case one quadrant of reciprocal space was collected and symmetry-related reflections were averaged. In the daunomycin case data were observed to 1.5-Å resolution; however, for the adriamycin crystal the data were weak between 1.5 and 1.7 Å, so that only those reflections to 1.7 Å observed at greater than $2\sigma(F)$ were used in the structure solution. These crystals were essentially isomorphous with the daun–TA complex (Wang et al., 1987), and the coordinates of that structure were used as starting models in each case. The central base pairs were adjusted for the change in sequence, and the structures were refined in steps of increasing resolution by using the Hendrickson–Konnert constrained least-squares refinement procedure (Hendrickson & Konnert, 1981) as modified for nucleic acids (personal communication from G. J. Quigley).

In each case, the DNA–drug complex is positioned on a crystallographic twofold axis, and one strand of the DNA and one drug molecule comprise the asymmetric unit in the cell. However, each structure was refined with lower symmetry by using all the atoms of the double-stranded complex, and then the symmetry-related atomic positions were averaged after each group of refinement cycles. Solvent molecules were located from a series of difference Fourier maps and gradually added, always in symmetry-related pairs, as the refinement continued. For the adriamycin structure, the additional hydroxyl at C14 was omitted during the initial stages of refinement. It was located as an extra lobe of difference density from the early Fourier maps and was, therefore, added in its proper location. In all three complexes, daun–TA, daun–AT, and adri–AT, one solvent molecule had a coordination structure consistent with that of a hydrated sodium ion. This six-coordinate molecule, which is within hydrogen-bonding distance of N7 of the 3′-terminal guanine, O4 and O5 of the anthracycline, and three water molecules, was refined as a sodium ion during the later stages of refinement.

Throughout the refinement, certain groups of water molecules remained poorly resolved and appeared as strings of electron density. These included areas close to DNA hydrogen-bond donors and acceptors which, on the basis of their shape and positions, might represent spermine molecules. To determine whether this solvent density was better represented as spermine molecules, we removed each in turn and subjected the structures to several cycles of refinement. Omit difference Fouriers supported this approach since the volumes and lengths of these strings of density matched that expected for spermine molecules. Therefore, we placed the distance-constrained carbon and nitrogen atoms of spermine into the strings of density. One spermine molecule was added per asymmetric unit to the daun–AT structure, and, independently, one was added to the adriamycin complex. After continued refinement, the positional and thermal shifts converged, and the R factors dropped to 17.7% in the adri–AT complex and 17.5% in the daun–AT complex. As a final test, these spermine molecules were then replaced with properly spaced water molecules, the structures refined again, and these "new waters" removed to calculate another set of difference Fourier maps. In both cases, the omit difference density had the appearance of spermine

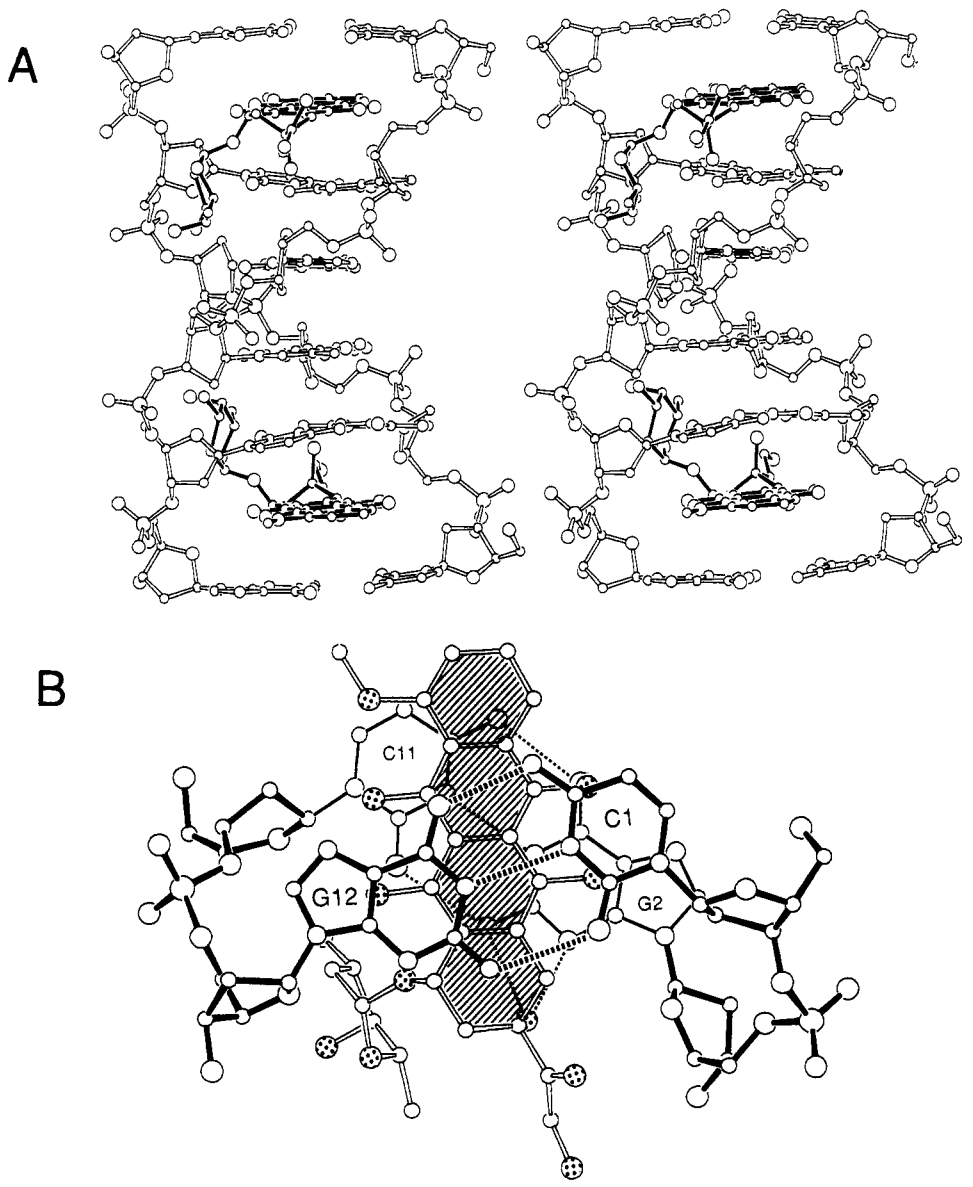

FIGURE 2: ORTEP representation of the adriamycin–CGATCG complex. (A) Stereoview of the complete molecule with the twofold axis horizontal. The DNA molecule is drawn with open bonds, and the two adriamycin molecules are drawn with solid bonds. The even separation between chromophore and base pairs gives the impression of an extended helix. (B) Projection onto the plane of the adriamycin chromophore. The terminal G–C base pair is drawn with thick solid bonds, the plane of the adriamycin rings is shaded, and the lower base pair is drawn with thin bonds. The oxygens of adriamycin are highlighted with stippling. In addition to the base-pair hydrogen bonds, the two hydrogen bonds from O9 of adriamycin to N2 and N3 of G2 are also drawn with dotted lines.

molecules rather than the individual refined water molecules. The final refinement of the adri–AT complex, using 1706 reflections from 10.0 to 1.7 Å with $F > 2\sigma(F)$, including 1 hydrated sodium ion, 1 spermine molecule, and 53 unique water molecules per DNA strand, had an rms deviation in bond lengths from ideal values of 0.028 Å. For the daun–AT complex with 2731 reflections from 10.0 to 1.5 Å [$F > 2\sigma(F)$], with 1 hydrated sodium ion, 1 spermine molecule, and 57 unique water molecules, the corresponding value was 0.036 Å. The atomic coordinates for both structures have been deposited in the Brookhaven Protein Data Bank.

RESULTS

Structure of the Complexes: (*a*) *Aglycon.* In all three drug–DNA complexes, daun–TA, daun–AT, and adri–AT, the aglycon moiety intercalates at the same sites in the DNA hexamers, between the G–C base pairs on either end of the duplex. A skeletal drawing of the complete adriamycin complex is shown in Figure 2A. The orientation of the aglycon and conformation of ring A, which fits cleanly into the electron density in each complex, are highly conserved throughout the series. It appears that neither the addition of a hydroxyl group to position 14 nor the change in DNA sequence adjacent to the intercalation site has an effect on the position of the aglycon.

A more detailed picture of the intercalation of the adriamycin aglycon between the two terminal base pairs can be seen in Figure 2B (the aglycon is shaded). In this view, the molecule has been rotated toward the viewer so that the three planar rings (B–D) of the drug define the plane of the paper. The base pairs above (thick solid bonds) and below (thin solid bonds) are projected onto this plane. The slightly skewed orientation of the aglycon relative to the two phosphate backbones is nearly identical with that reported previously in the daun–TA complex (Quigley et al., 1980; Wang et al., 1987) and appears to be determined by anchoring interactions on each end of the aglycon. The hydrogen-bonding interactions between the DNA and both adriamycin and daunomycin are

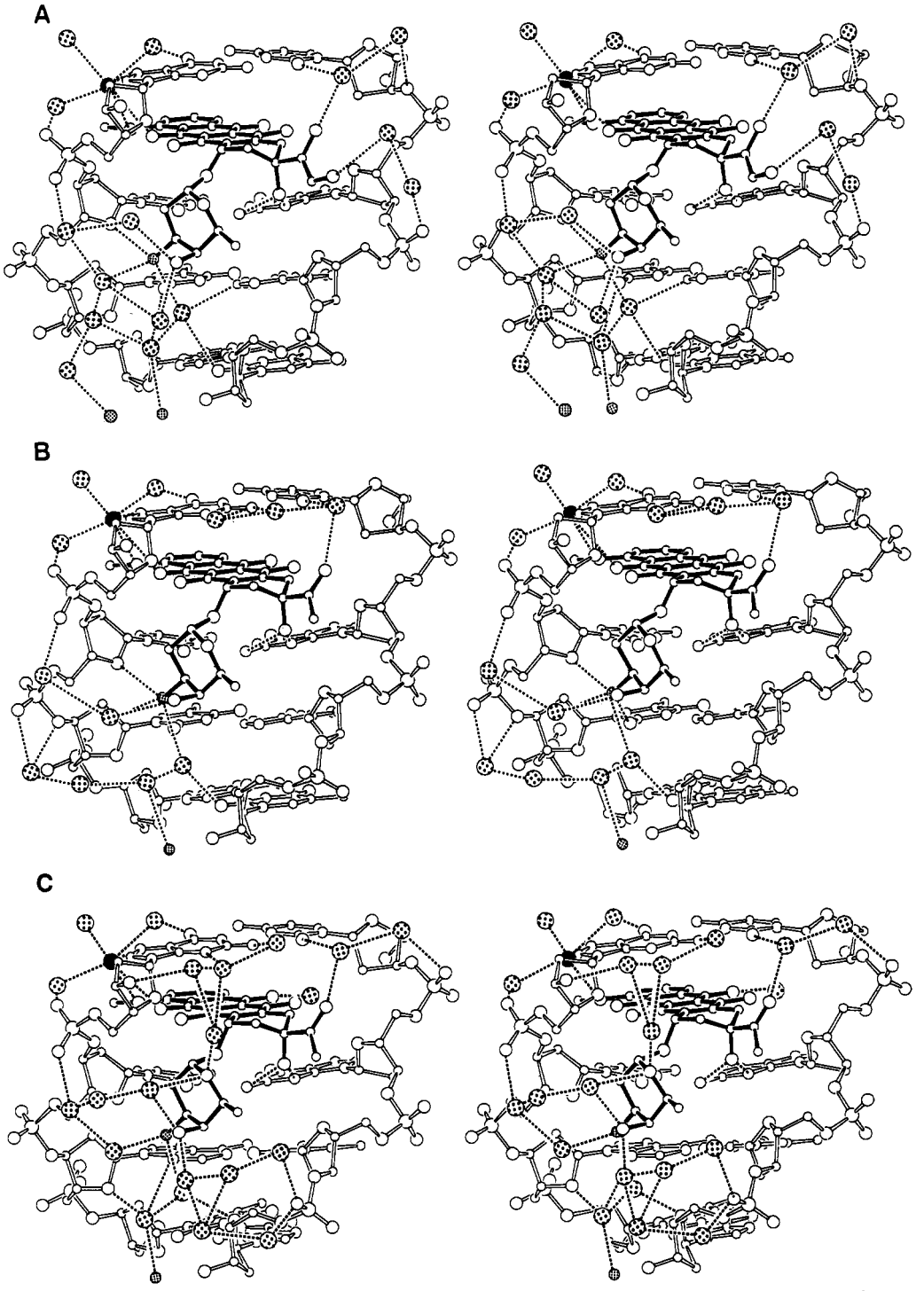

FIGURE 3: Stereoviews of the hydrogen-bonding interactions between adriamycin (A) or daunomycin (B) and the DNA fragment d(CGATCG) and (C) daunomycin with d(CGTACG). In each panel the DNA is drawn with open bonds, the drug is drawn with solid bonds, bridging water molecules are stippled. In addition, the conserved sodium ion that helps to stabilize the DNA–drug interaction is shown as a solid sphere. All hydrogen bonds are drawn as dotted lines. The amino sugar N3′ atoms of both drugs as well as each symmetry equivalent N3′ atom are shaded and are shown bridged by two symmetry-related water molecules.

illustrated in Figure 3. For comparison we have included a similar view of the original daun–TA complex as well. The dashed lines represent hydrogen bonds formed directly and through bridging solvent molecules to the DNA.

In each complex, one end of the aglycon is anchored by two direct hydrogen bonds between the drug and the DNA. These hydrogen bonds, from O9 of anthracycline to N2 and N3 of residue G2, are highly conserved in the series of three complexes. The position of this end of the drug is also stabilized by an indirect hydrogen bond from O13 of the drug through one bridging water to O2 of the terminal cytosine residue. In all three complexes, the other end of the aglycon is anchored by coordination to a solvent molecule that appears to be a sodium ion. This solvent molecule forms direct hydrogen bonds to oxygens O4 and O5 of the aglycon and is also directly coordinated to N7 of G12. The position of this solvent molecule is firmly fixed by two additional water ligands which bridge to the DNA, one to O6 of G12 and one to the phosphate oxygen O1P of this residue. This complex set of interactions provides a striking example of highly specific stabilization of drug–DNA complexes by a solvent molecule.

In addition to this set of conserved interactions, similar

patterns of bridging solvent interactions from drug to DNA backbone are observed in each complex. In the two AT complexes, crescent-shaped strings of water molecules extend from the N3′ of the amino sugar to phosphate oxygens of one strand. In the daun–TA complex a similar crescent of water molecules extends from N3′ to the other strand. The daun–TA complex contains additional water-bridged contacts to the DNA. The bridge stretching upward from the amino sugar may explain the different position of that sugar in this complex.

In the vicinity of the extra hydroxyl group of adriamycin, there are specific differences in solvation as compared to the other two complexes. The positions of solvent molecules are shifted such that in the adriamycin complex there are bridging interactions to phosphate groups of the proximal DNA strand, while in both the daun–AT and daun–TA complexes there are several water molecules interacting with the minor groove edges of the terminal base pair.

(*b*) *Amino Sugar.* The anthracycline amino sugar, in contrast to the aglycon and the DNA, shows different conformations and interactions in this series of three complexes. Although the amino sugar extends into the minor groove in each of the three complexes, there are conformational differences caused by the change in DNA sequence. The interactions of the amino sugar moiety with DNA are different in the daun–TA complex from the two AT complexes (adri–AT and daun–AT). In the AT complexes, the amino sugar lies closer to the deoxyribose and base edge of residue C11. This change in conformational is caused by the change in DNA sequence at the next base pair. When the aglycon of daun–AT is superimposed onto the aglycon of adri–AT, the atoms in the flanking surrounding base pairs plus those of the amino sugars of the drugs maintain a close fit, with a root mean square deviation of only 0.15 Å. However, when the aglycon of daun–AT is superimposed onto the aglycon of daun–TA, the same atoms form a worse fit with a root mean square deviation of 0.35 Å.

In comparison with daun–TA, the amino sugars in the two AT complexes form more favorable interactions with the DNA. The van der Waals and hydrogen-bond distances are significantly shorter. Thus, a switch of the central base pair of daun–TA appears to increase the stability of the complex. In the AT complexes, but not the daun–TA complex, the N3′ of the amino sugar forms direct hydrogen bonds to the minor groove of the DNA. In the AT complexes, five potential hydrogen-bond acceptors, O4′ and O2 of residue C11, O2 of residue T10, and two water molecules, are within 3.3 Å of the N3′. We assume that this positively charged functional group can only form three hydrogen bonds. Although the angle to O2 of C11 appears to be unfavorable, from our data, it is not possible to disqualify any of the other four and, therefore, all four have been included in Figure 3. In contrast, in the daun–TA complex, the distance from N3′ to any potential hydrogen-bond acceptor on the DNA is greater than 3.5 Å, too long for a hydrogen bond. However, the two hydrogen bonds from N3′ to solvent molecules are conserved in all these complexes (Figure 3). Note that in these structures, which diffract to resolutions of from 1.2 to 1.7 Å, hydrogen atoms are not observed and hydrogen bonds are inferred from distances between electronegative atoms and their geometries. Under these circumstances, the definition of a hydrogen bond is necessarily subjective. We have used 3.3 Å as a hydrogen bond cutoff. However, our conclusions regarding the relationship between DNA sequence and stability (below) are independent of the definition of a hydrogen bond.

In the two AT complexes, the amino sugar makes several van der Waals contacts with the edges of the base pairs within the minor groove. The individual atoms making up one side of the amino sugar, C2′, C3′, and C4′, are between 2.7 and 3.4 Å from both the adjacent cytosine and T–A base pair. This tight fit of adri–AT can be seen in Figure 4A, where the van der Waals surface of the shaded amino sugar nests against the A3–T10 base pair. In Figure 4B the same view for the daun–TA complex shows a slightly greater separation of the amino sugar from the DNA.

DNA Conformation. The DNA conformation in these complexes is surprisingly regular, with only minimal deviations of backbone torsion angles from standard B conformation, even at the site of intercalation. Thus, the DNA backbones have the appearance of extended B-DNA-like helices. However, specific changes in B-DNA conformation accompany the intercalation of these large drug molecules. The major deviations from the B-DNA conformation are found at the intercalation sites and can be seen in Figure 3. In this view looking directly into the minor groove, the base pairs above and below the intercalator are significantly buckled (see Table II). In each complex, the C–G base pair above the chromophore is buckled by approximately 9°, while the G–C base pair below the chromophore, i.e., within the helix, has a larger buckle of approximately 15° in the opposite direction. As listed in Table I, there are asymmetric changes in backbone torsion angles on either side of the intercalator, giving a base-pair helical rise, (C1′ to C1′), of 5.2 Å at this site as compared to 3.5 Å for the other steps along the DNA. These distortions combine to result in an increase in the base-pair separation to almost two "normal" B-DNA base-pair steps. The terminal C–G base pairs are displaced relative to the helix axis by 2.7 Å in the direction of the minor groove. This is significantly greater than the average seen in B-DNA. However, the global helical twist values for these complexes are very close to fiber B-DNA. In addition, the terminal base pairs have low roll values, −0.5° and −1.0° for the adri–AT and daun–AT, respectively, preventing steric clashes with the inserted chromophore. A more complete listing of helical parameters for all three complexes is given in Table II.

The usual ζ/α phosphodiester linkage conformation of B-DNA of gauche$^-$/gauche$^-$ is observed for most residues in the present complexes (see Table I). However, there are two exceptions, at the G2pA3 step and the C5pG6 step, where ζ values have been increased to trans conformations of 179° and 171° (values are average for three complexes), respectively. In each case this motion is coupled with at least one other angular shift. The ϵ for residue C1 is reduced to 229°, and the glygosyl linkage is rotated so that it is in a low anti conformation. Also, the average β value for residue A3 of 141° is considerably smaller than found in the rest of the duplex. The increase in base-pair separation on the opposite strand, however, is caused by a reduction in ϵ on the 5′ side of the intercalation site to an average of 258°, very different from the usual near trans conformation. These coupled torsional rotations shift the attached base roughly along the direction of the helix axis and maintain base-pairing geometry.

In this way the phosphate conformation is extended on the amino sugar side of the chromophore while the guanine with which the O9 substituent atom is hydrogen bonding is pulled out and downward as well. This has the net effect of pushing the base pair on the 3′ side of the chromophore toward the major groove, as compared to the base pair above it.

Two adjacent base-pair steps along the helix are shown, in projection in Figure 5. In both the daun–TA and adri–AT

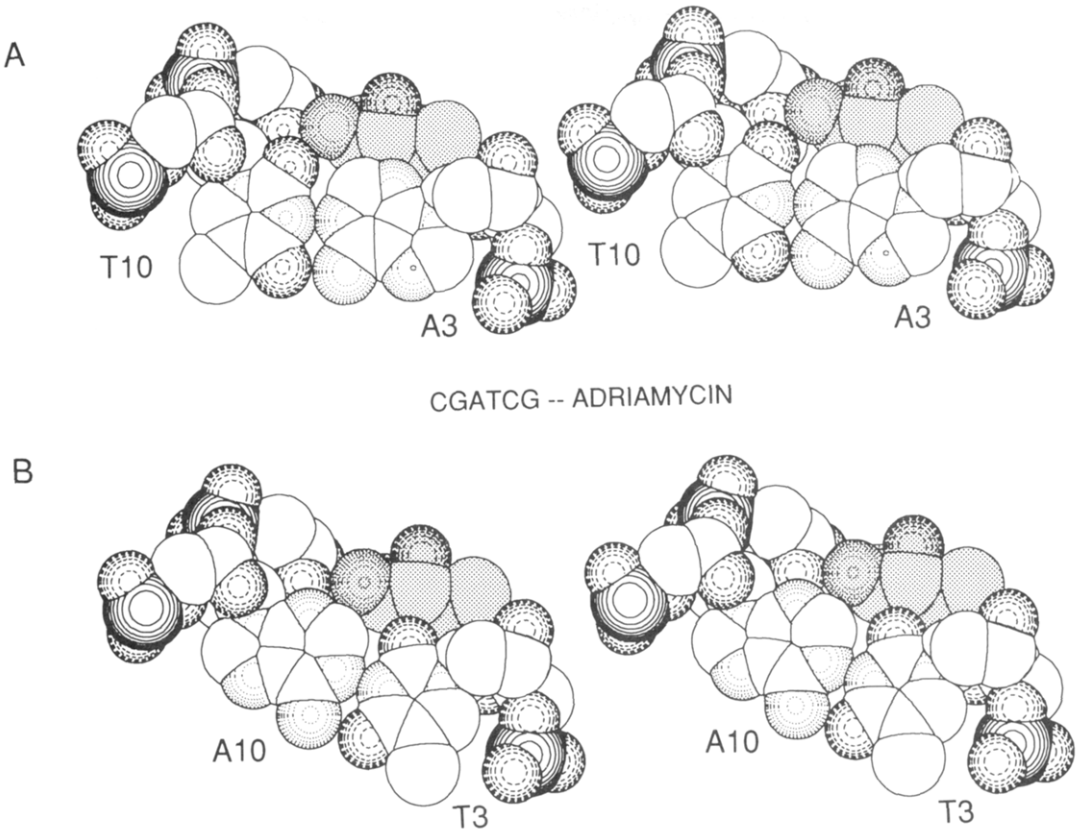

FIGURE 4: Stereo van der Waals surfaces showing the interactions of the amino sugar with the DNA A–T base pair as viewed looking down onto the A–T base pair. Oxygen atoms are drawn with dashed shading, nitrogens with dotted shading, and carbons as open spheres. The entire amino sugar moiety is shaded in both panels to emphasize its fit against the base pairs. (A) From the adriamycin–CGATCG structure, the base pair A3–T10 and attached backbone ribose, viewed so that the amino sugar is now below the DNA base pair. Two hydrogen bonds are formed from the N3′ of the amino sugar to the thymine O2 and the adjacent ribose O4′. The close fit of the N3′ atom between these two oxygen atoms is clear from this view. (B) Same view from the daunomycin–CGTACG structure. The entire sugar is slightly farther away from the base pair, so that the fit of the sugar N3′ between the adenine N3 and ribose O4′ is not as close as in (A).

Table I: Backbone and Glycosyl Torsion Angles (Degrees) and Sugar Conformations[a]

residue	α	β	γ	δ	ϵ	ζ	χ	P	ribose pucker
				Adriamycin–d(CGATCG) Complex					
C1(C7)			37.0	138.0	226.5	291.2	211.9	158	C2′-endo
G2(G8)	269.5	184.4	55.8	130.7	216.9	180.1	268.9	141	C1′-exo
A3(A9)	318.3	134.8	35.4	130.2	187.2	264.7	230.1	129	C1′-exo
T4(T10)	298.3	171.8	53.4	122.1	200.2	268.3	246.7	124	C1′-exo
C5(C11)	301.6	162.2	34.9	143.4	259.8	170.4	272.4	151	C2′-endo
G6(G12)	301.9	172.4	35.9	145.4			271.9	161	C2′-endo
				Daunomycin–d(CGATCG) Complex					
C1(C7)			32.8	151.6	233.1	287.2	209.6	160	C2′-endo
G2(G8)	282.6	175.6	50.0	139.0	223.5	178.2	264.7	142	C1′-exo
A3(A9)	291.8	147.9	51.5	124.1	181.0	267.2	225.9	131	C1′-exo
T4(T10)	283.1	180.9	64.2	121.5	198.7	263.9	246.9	122	C1′-exo
C5(C11)	311.4	159.7	31.2	139.5	255.7	171.7	275.5	141	C1′-exo
G6(G12)	301.6	167.6	41.0	144.5			272.4	165	C2′-endo
				Daunomycin–d(CGTACG) Complex					
C1(C7)			45.5	141.6	228.3	292.5	205.9	157	C2′-endo
G2(G8)	291.2	175.9	36.4	146.0	210.2	177.6	274.3	152	C2′-endo
T3(T9)	310.9	138.4	50.5	116.2	186.4	275.3	223.7	105	O4′-endo
A4(A10)	278.8	182.1	59.2	131.3	190.7	269.4	257.6	147	C2′-endo
C5(C11)	298.1	172.9	31.7	143.1	255.6	171.7	272.4	136	C1′-exo
G6(G(12)	292.3	174.0	47.3	144.5			273.9	182	C3′-exo
A-DNA	290	172	41	79	214	282	206		C3′-endo
B-DNA	327	138	33	142	219	203	221		C2′-endo

[a] Torsion angles along the backbone of the oligonucleotide are defined as $P\text{–}O5'\overset{\alpha}{\text{–}}C5'\overset{\beta}{\text{–}}C4'\overset{\gamma}{\text{–}}C3'\overset{\delta}{\text{–}}O3'\overset{\epsilon}{\text{–}}P\overset{\zeta}{\text{–}}$ and χ is the glycosyl angle.

complexes, the stacking interactions at these steps are much like those of B-DNA. In this section the adri–AT is compared to daun–TA to contrast a purine–purine step with a purine–pyrimidine step. For example, in the upper left of Figure 5

Table II: Helical Parameters for DNA–Drug Complexes[a]

base pair	roll	tilt	inclin	prop tw	buckle	helic tw	rise
			Adriamycin–d(CGATCG) Complex				
C1–G12	−1.00	−0.62	3.45	−1.42	−9.28	34.95	5.231
G2–C11	−1.28	−2.35	11.99	−1.25	14.95	32.68	3.469
A3–T10	3.08	−0.01	12.24	−3.64	6.70	32.13	3.531
T4–A9	−1.28	2.35	12.24	−3.64	−6.70	32.68	3.469
C5–G8	−1.00	0.62	11.99	−1.25	−14.95	34.95	5.231
G6–C7			3.45	−1.42	9.28		
av	−0.30	0.00	9.22	−2.10	0.00	33.47	4.19
sd	1.89	1.72	4.47	1.19	11.91	1.36	0.95
			Daunomycin–d(CGATCG) Complex				
C1–G12	−0.45	−0.44	4.00	−1.44	−9.42	35.36	5.142
G2–C11	−0.42	−3.33	12.17	−0.07	16.18	31.56	3.545
A3–T10	0.03	0.00	11.32	−3.09	6.34	31.99	3.365
T4–A9	−0.42	3.33	11.32	−3.09	−6.34	31.56	3.545
C5–G8	−0.45	0.44	12.17	−0.07	−16.18	35.36	5.142
G6–C7			4.00	−1.44	9.42		
av	−0.34	0.00	9.16	−1.53	0.00	33.17	4.15
sd	0.21	2.37	4.02	1.36	12.50	2.01	0.91
			Daunomycin–d(CGTACG) Complex				
C1–G12	−1.63	−0.67	2.90	−0.59	−8.13	34.95	5.277
G2–C11	−3.83	−1.43	9.33	−2.00	16.36	30.85	3.362
T3–A10	8.00	0.00	9.07	−6.79	3.68	34.48	3.695
A4–T9	−3.83	1.43	9.07	−6.79	−3.68	30.85	3.362
C5–G8	−1.63	0.67	9.33	−2.00	−16.36	34.95	5.277
G6–C7			2.90	−0.59	8.13		
av	−0.58	0.00	7.10	−3.13	0.00	33.22	4.19
sd	4.92	1.12	3.26	2.90	11.79	2.17	1.00

[a] These parameters were obtained from the program NEWHELIX, provided by R. E. Dickerson and colleagues and are in accordance with EMBO workshop guidelines (Dickerson et al., 1989).

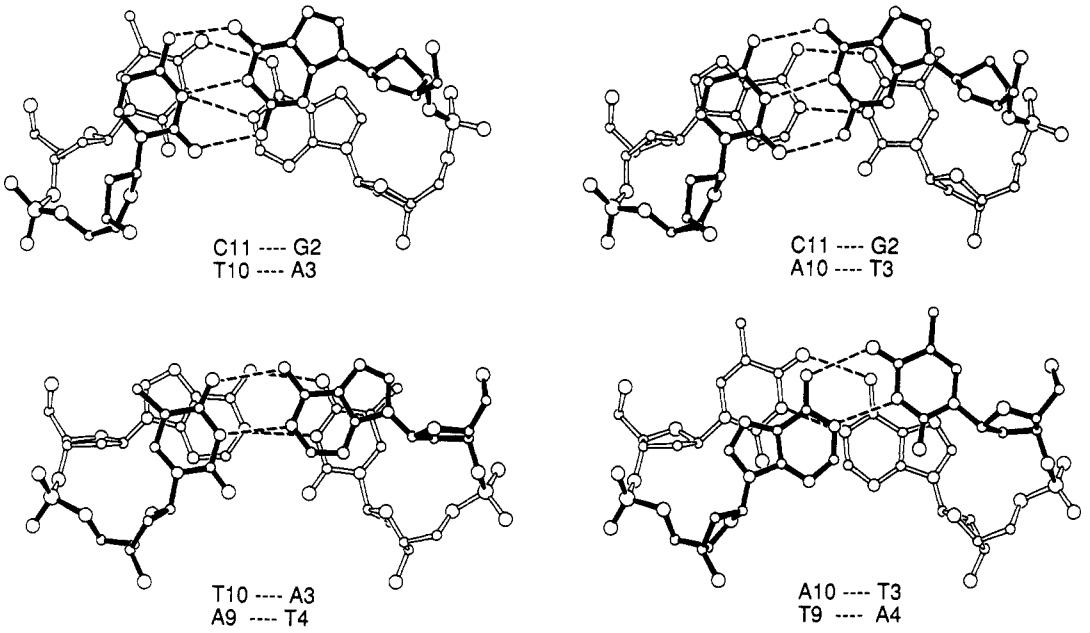

FIGURE 5: Comparison of base-pair steps from adriamycin and daunomycin structures. Panels on the left are from the adriamycin–CGATCG structure; those on the right are the analogous steps from the daun–TA structure. The view is down onto the plane of the lower base pair, with the upper bases drawn with solid bonds. Base-pairing hydrogen bonds are shown with dotted lines.

(panel A), the adenine N6 in the adriamycin complex and the thymine O4 in the daunomycin complex are almost directly beneath their respective guanine six-membered rings. This figure also illustrates some subtle differences in the two complexes. The adriamycin A3–T10 base pair has slightly more buckle (~7°) than the corresponding T3–A10 pair in the daunomycin complex, which instead has a slightly higher propeller twist angle of −7°. The position of the complex on a crystallographic twofold axis requires that A3–T10 and T4–A9 base pairs have the same amount of buckle (about 7°). In contrast, the symmetrical propeller twist of the other A–T base pair in the daunomycin complex can be seen in these panels as well.

Recently there has been a great deal of interest in differences between ApT versus TpA base steps (Ulanovsky & Trifonov, 1987; Diekmann, 1987; Burkhoff & Tullius, 1988). These anthracycline complexes allow a direct comparison of ApT to TpA steps in otherwise very similar structures. Several consistent differences between these two types of steps in other lower resolution B-DNA crystal structures (Yoon et al., 1988; Coll et al., 1989) are also observed in these complexes. In both AT complexes the helical twist for the ApT step is ~32°, while

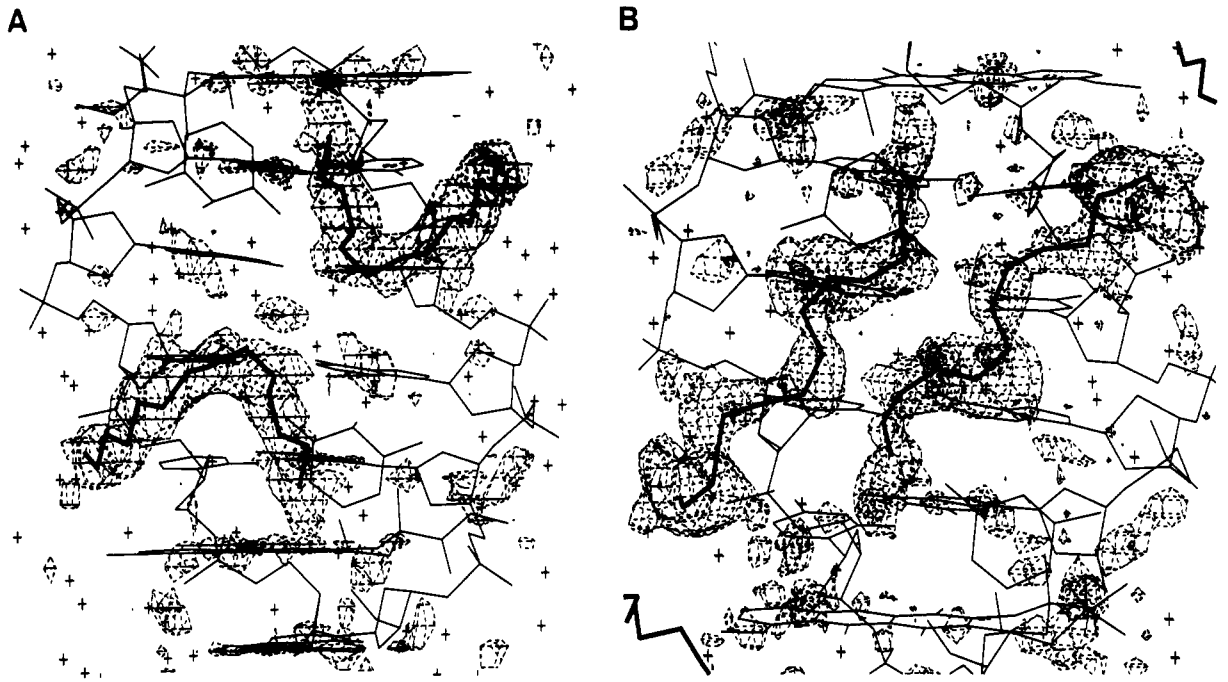

FIGURE 6: Omit density maps for the adriamycin and daunomycin spermine molecules. (A) View looking into the major groove of the adriamycin complex. (B) Corresponding view from the daunomycin complex. In both panels the omit density contoured at 2σ is drawn as a thin mesh, the DNA backbone is drawn with thin lines, and the spermine atoms are drawn with heavy lines.

in the daun–TA structure the twist for the TA step is just slightly larger at 35°. Sequence-dependent variations in this angle were also seen in an earlier A-DNA alternating AT structure, although the actual differences were the reverse of what we observe here (Shakked et al., 1981, 1983). The present comparison also shows less positive base-pair roll in the ApT steps (0.5 or 0.0°) than for TpA (8°) in daun–TA, where a pyrimidine–purine stack is opening toward the minor groove to avoid cross-strand clashes. Conversely, the central base pairs show more propeller twist in the daun–TA complex than is seen in the AT complexes. Finally, in the ApT steps, there is good intrastrand base overlap for both strands. In the TpA step (in the daun–TA complex), however, the thymine is pulled out of the stack toward the major groove, coupled with a very low pseudoratation value for the thymine residue.

Solvent Interactions. The quality of the $2F_o - F_c$ electron density maps for both the adriamycin and daunomycin structures are very good, as expected for well-refined, high-resolution structures. The electron density corresponding to the solvent molecules is also well resolved, providing a high level of confidence in the positions of these solvent molecules. In all three complexes the N3′ of the amino sugar forms water-mediated hydrogen bonds to the floor of the minor groove. In the AT complexes, the hydrogen-bond acceptor is the O2 of T4. In the daun–TA complex, the hydrogen-bond acceptor is the N3 of A4. With these water-mediated hydrogen bonds, the symmetry-related amino sugars are linked through their N3′ atoms by two symmetry-related bridging water molecules, as shown in Figure 3. The two symmetry-related O4′ atoms in the adri–AT complex are also linked by symmetry-related water molecules, which have been included in Figure 3A as well.

In the adri–AT complex, the amino sugar N3′ forms a multiple water bridge to a backbone phosphate oxygen. Two analogous connections are observed in daun–AT, where fewer water molecules bridge to two phosphate groups. Finally, the adriamycin 14-hydroxyl group is involved in a bridge to a phosphate oxygen, again through two intermediate water molecules. One of these water molecules is in turn hydrogen bonded to the end of the spermine from an adjacent symmetry-related complex (below).

One clear difference in the solvent organization of adri–AT versus daun–AT involves the two spermine molecules (which are related by twofold symmetry) bound to each duplex. Parts A (adri–AT) and B (daun–AT) of Figure 6 show sections of the omit difference Fourier maps contoured at 2σ above background. Both sets of spermine molecules can be easily located within their respective cages of electron density. The positions of these spermine molecules with respect to the DNA helix are shown in Figure 7 and in more detail in Figure 8.

In the adri–AT complex (Figure 8A), the crescent-shaped spermine spans the major groove near the center of the duplex. It extends from near the 5′ sugar of one strand, past the edge of the base of G2, dips down near the next A–T base pair, and curves up again near the phosphate group of T10 on the opposite strand. In this complex, the spermine molecules do not form direct hydrogen bonds to the DNA. However, both ends form hydrogen bonds through bridging water molecules to backbone oxygen atoms. The central atoms of these spermine molecules are in van der Waals contact with the edges of the central base pairs. The two spermine molecules almost completely fill the major groove in this region.

In the daun–AT complex a different spermine position was identified. As shown in Figure 8B it is located in the major groove in the center of the duplex, in analogy with the spermine molecules of the adri–AT complex. However, in contrast to the adri–AT complex, the spermine molecules in the daun–AT complex assume an extended conformation and stretch lengthwise along the groove. The two nitrogens at one end make direct hydrogen bonds to N7 of guanine and to N7 of the neighboring adenine. The next nitrogen is hydrogen bonded through two bridging water molecules to a phosphate oxygen, and the last nitrogen forms hydrogen bonds to another phosphate oxygen, through a bridging water. As in the adri–AT complex, the central carbon atoms of spermine are in van der Waals contact with the base-pair edges. In this orientation as well, the two symmetry-related molecules (Figure 8B) nearly fill the major groove, but in a conformation

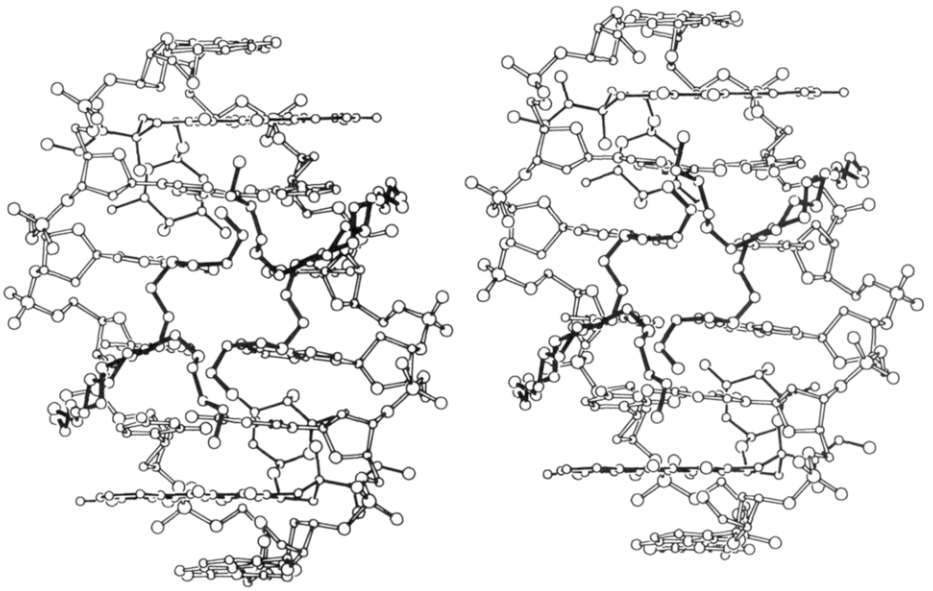

FIGURE 7: Stereo ORTEP representation of the spermine molecules associated with both structures. The spermine atoms from the daun–AT complex were superimposed onto the adriamycin complex, including its own spermine molecules. The DNA and intercalated drug molecules are shown with open bonds and the two sets of symmetry-related spermine molecules with solid bonds.

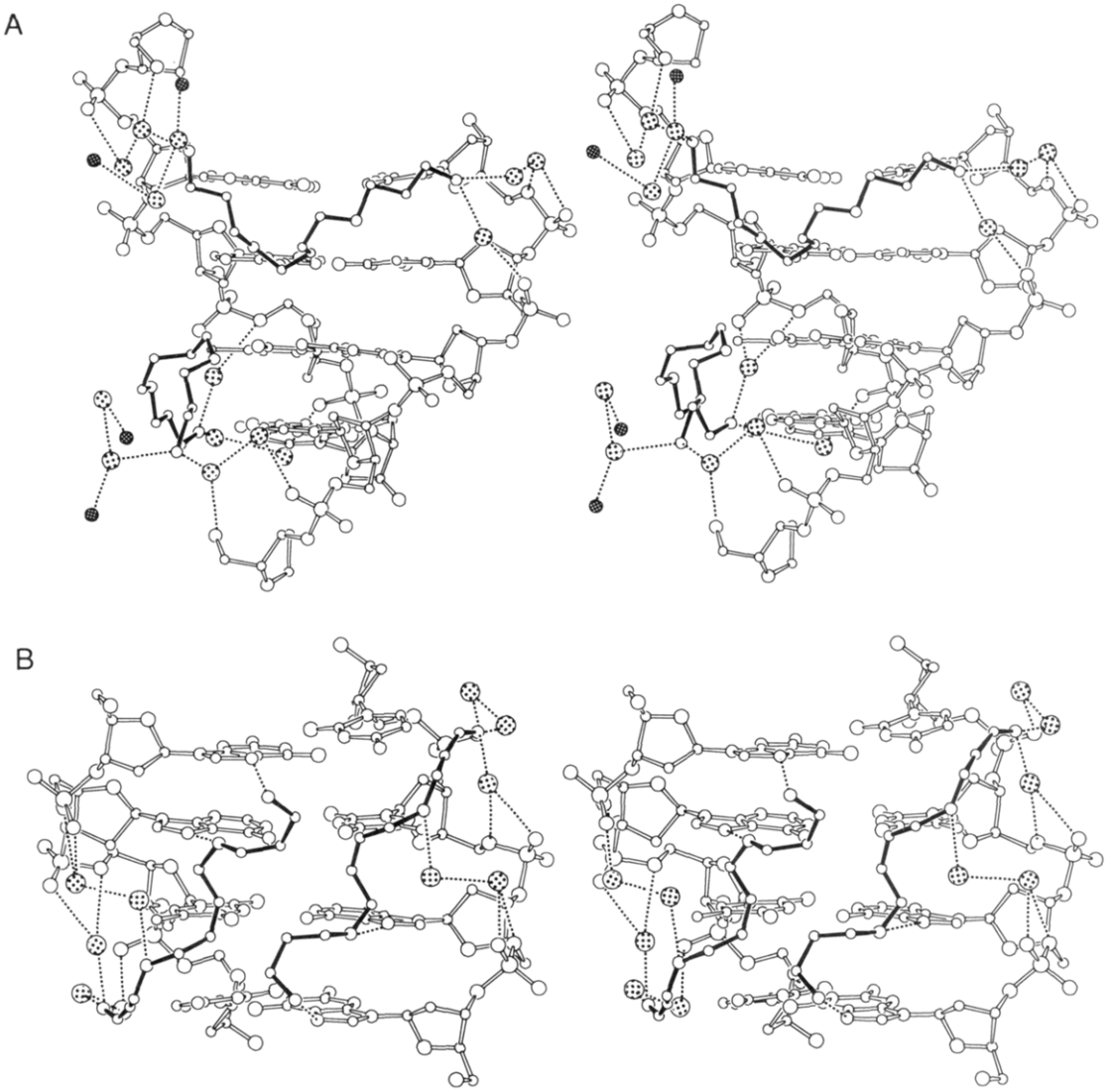

FIGURE 8: Detailed stereoviews of the spermine molecules associated with the (A) adriamycin– and (B) daunomycin–CGATCG complexes. In each panel the spermine molecules are drawn with solid bonds; the sections of the DNA helix with which they interact are drawn with open bonds. In both panels bridging water molecules are stippled, and in (A) the symmetry-related DNA oxygen atoms to which spermine molecules are bridging are also shown with dark shading.

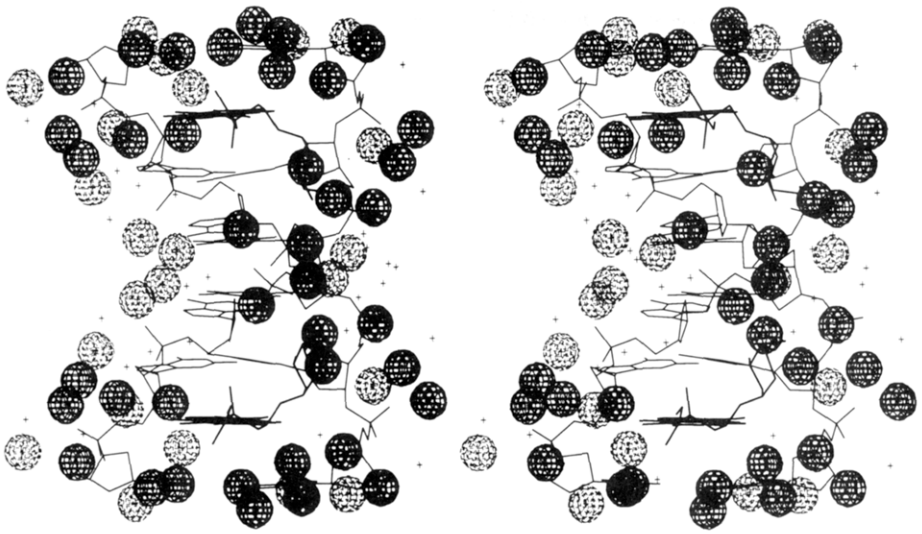

FIGURE 9: First-shell solvent interactions conserved in the adriamycin and daunomycin structures. The solvent molecules that are present in the same position (within 1.0 Å) in all three structures are represented by the van der Waals surfaces drawn with dark lines. Those drawn with lighter lines correspond to the positions that are conserved in only two of the three structures. The small crosses represent positions of other unique solvent molecules from the three individual structures.

that is very different from that of the daun–AT structure.

In Figure 7, the spermine molecules from both complexes are superimposed onto the adri–AT complex. Although the positions of individual spermine atoms of daun–AT are significantly different from those of adri–AT, the independently refined spermine molecules overlap for about half of their respective lengths. In total, the spermine molecules from the two different complexes fill nearly the same region. It is important to note that at the point where the molecules from the difference complexes diverge there was no difference density corresponding to the location of the other conformation in either respective $2(F_o - F_c)$ Fourier map.

Despite significant differences in the spermine conformations and interactions, and the water molecules in their vicinity, the solvent arrangement in other regions of these complexes is generally well conserved. Figure 9 shows a comparison of the first-shell solvent atoms from both daunomycin structures superimposed onto those of the adri–AT complex. It is clear that many water molecules in the three independently refined structures are located at nearly identical positions. At certain locations, a nitrogen atom from a spermine falls almost exactly on a water position from the other two structures. Those water molecules from the adri–AT complex that are fully conserved in the series of three drug–DNA complexes are shown as dark spheres in Figure 9, while the water molecules from the adri–AT complex that are conserved in only two of the three complexes are shown as dashed spheres. Generally, there are at least two solvent molecules close to the phosphate oxygens as is typical of B-DNA (Saenger et al., 1986). The water molecules around the phosphate oxygens and the ends of the helices (forming lattice contacts) are highly conserved.

Discussion

The solution of three analogous DNA–drug complexes, adri–AT, daun–AT, and daun–TA, provides a basis for understanding the effects of drug modification and DNA sequence on structure and stability of these complexes. This paper describes the three-dimensional structures of adriamycin and daunomycin complexed to the DNA hexamer, CGATCG, while the structure of daunomycin in another sequence, CGTACG, was previously reported from this laboratory (Quigley et al., 1980; Wang et al., 1987). In this series of complexes we observe both conserved interactions (which appear to be universal to this class of DNA–drug complex) and sequence/modification-specific interactions. The DNA conformations, including backbone torsion angles and sugar puckers, are very similar, and the three DNA molecules are almost superimposable. Similarly, the position of the anthracycline aglycon, intercalated between two G–C base pairs, is conserved. In each structure, one end of the aglycon is anchored by a solvent molecule that appears to be a sodium ion. This six-coordinate molecule is bichelated by the O4 and O5 oxygens of the aglycon and also to the major groove of the DNA, directly coordinated to N7 of guanine. The other end of the aglycon is anchored by two direct hydrogen bonds from the O9 hydroxyl of the drug to the DNA within the minor groove. The conservation of these hydrogen bonds is consistent with biochemical evidence that in solution the O9 hydroxyl is required for activity (Henry, 1979). An additional hydrogen bond (via a bridging water molecule) from the O13 of daun–TA and daun–AT to O2 of residue C1 is also observed in adri–AT. However, this is in the region of the distinguishing O14 hydroxyl, where the organization of the solvent molecules associated with adriamycin is different from that of the two daunomycin complexes. This O13 of adriamycin also forms another hydrogen bond through two bridging water molecules to O3′ of the terminal base pair, while in the daunomycin complexes the bridging interaction is to the guanine N3 atom of this base pair instead.

In contrast to the strongly conserved interactions of the fused ring system, the positions and interactions of the anthracycline amino sugars show subtle, but significant, variation in this series of complexes. In all three complexes, the amino sugar lies in the minor groove. However, this positively charged moiety appears to form a tighter complex with CGATCG than with CGTACG. In daun–TA, the amino group does not form hydrogen bonds to the DNA. However, in daun–AT, and adri–AT the amino sugar is shifted significantly toward the floor of the minor groove and lies within hydrogen-bonding distance of the O4′ and O2 of C11 and the O2 of T10. These structures are consistent with DNA base-triplet specificity, 5′-CGN, previously discussed for anthracycline binding in solution (Chen et al., 1986; Chaires et al., 1987).

Solvent molecules form an integral part of these drug–DNA complexes. As mentioned above, a solvent molecule appears to be a sodium ion and certain water molecules form conserved

bridging interactions between the drug and nucleic acid. These interactions underscore the importance of water molecules and ions in determining the specificity and stability of the complexes. Throughout the series, comparisons of the overall hydration patterns show that the locations and interactions of the first solvent shell are generally conserved. In the minor groove, there are two well-ordered water molecules per duplex which form an abbreviated spine (Drew & Dickerson, 1981). When the central sequence is switched from TpA to ApT, the spine is conserved; the hydrogen-bond-acceptor site of the DNA changes from N3 of adenine to O2 of thymine. The organization of solvent around phosphate oxygens is typical of B-DNA, with two water molecules generally bridging between adjacent residues (Saenger et al., 1986). Within the major groove, the spermine molecules have displaced water molecules.

The number and orientation of spermine molecules is a highly variable feature of these three complexes. No spermine molecules could be located in daun–TA. However, in daun–AT and adri–AT, two spermine molecules per duplex were located in the major groove. In daun–AT, the spermine molecules assume an extended conformation and are oriented parallel to the helical axis along the floor of the major groove. In contrast, in adri–AT, the spermine molecules form a crescent shape to span the width of the major groove. In both structures terminal amino groups of the spermine molecules interact with DNA phosphate oxygens through bridging water molecules, while in daun–AT two direct hydrogen bonds with purine N7 positions on adjacent base residues are formed with the other spermine nitrogens. Although the region of space occupied by the spermine molecules is essentially the same for daun–AT as for adri–AT, the specific spermine orientations and contacts vary. The distinguishing 14-hydroxyl of adriamycin interacts indirectly (via intervening water molecules) with the spermine and could in part explain the difference in spermine orientation. The difference in clinical activity of these antibiotics might be related to the changes in solvent environments caused by altering the drug's substituents. It is also possible that other molecules might interact with the additional hydroxyl group of adriamycin. This or other hydrophilic sites may provide other daunomycin derivatives with improved hydrogen-bonding potential. The pattern of drug interactions with a variety of biological targets, including not only nucleic acids but also soluble proteins or membrane components, may depend on a series of solvent-mediated interactions. Spermine molecules are flexible, and in these complexes they appear to have assumed different conformations on the basis of the drug and the DNA with which they are interacting. Since the concentration of spermine in the nucleus is several millimolar, these ternary complexes may be representative of the drug as bound to DNA in vivo. The different spermine complexes provide different surfaces for potential interactions with cellular proteins. In one case contacts to the hydrogen-bonding groups in the major groove would be altered, while in the second complex the interaction of molecules whose recognition mechanism depends on DNA groove shape would change.

The spermine molecules associated with these complexes provide models for the interaction of polyamines with B-DNA. Previously, a spermine molecule was tentatively identified in the dodecamer structure of Dickerson and colleagues (Wing et al., 1980) but at somewhat lower resolution than observed here. In that structure, the spermine molecule curves across the major groove much as we have observed in the adri–AT structure. In Z-DNA, where the very high resolution of the diffraction data allows precise location of almost all solvent atoms, there are also two spermine conformations (Wang et al., 1979; Gessner et al., 1989). One curves along the surface of the groove, while the other is extended and involved in lattice interactions. The hydrogen-bonding pattern is much the same as observed in the present structures, forming hydrogen bonds via bridging water molecules to phosphate oxygens or directly to guanine N7 atoms. Recently, a spermine molecule was described in an A-DNA octamer (Jain et al., 1989). In this complex, the spermine binds in the major groove and assumes an extended conformation forming hydrogen bonds directly to base residues in a manner similar to that seen in the daun–AT complex.

This series of complexes begins to provide a general overview of an intercalation site in a B-DNA helix. In these structures, the base pairs adjacent to the site of intercalation show large buckle and/or propeller twist. These deviations from planarity appear to result from the tendency to maintain stacking contacts between the intercalative moiety of the drug and the flanking base pairs. When the long axis of the stacked surface of the drug is nearly perpendicular to the long axis of an adjacent base pair (for example, the C1–G12 base pair, Figure 2B), then that base pair buckles to maximize van der Waals contact. However, when the long axis of the stacked surface of the drug is skewed to 45° from the long axis of an adjacent base pair (for example, the G2–C11 base pair, Figure 2B), then that base pair propeller twists to maximize contact. The base pairs buckle or twist to wrap around the intercalator. The relative extent of buckle and propeller twist is determined primarily by the orientation and shape of the intercalator. It is interesting to note that this phenomenon provides a reasonable physical basis for nearest-neighbor exclusion of intercalators. A base pair can only wrap in one direction at a time. This nonplanarity of the base pairs adjacent to the intercalation site is not an artifact caused by lattice forces. We have solved the structure of another daunomycin derivative complexed to a similar hexamer which has crystallized in a different lattice. Here the lattice interactions are necessarily different, and yet the same patterns of buckle and twist are observed (to be published elsewhere).

Conclusions

In the present paper we have made two structural comparisons, daunomycin bound to two different DNA sequences and two similar antitumor drugs, adriamycin and daunomycin, bound to the same DNA sequence. From the former comparison we learn that sequence changes outside the intercalative site have significant differences in terms of both the hydrogen bonding of the amino group on the sugar as well as the van der Waals interaction between the sugar and the minor groove of DNA. This means that the drug undoubtedly selects certain sites for binding over others.

The comparison of adriamycin and daunomycin binding to the same sequence reveals a subtle difference. We would expect, of course, additional interactions involving the solvent with the hydroxyl group on C14 of adriamycin. What was unexpected was the apparent influence of this altered solvent binding on the organization of bound spermine molecules, which differ in significant ways. Is this an explanation of the considerable differences in clinical use, where daunomycin is effective in human leukemias, while adriamycin is used for a variety of solid tumors? We do not know the answer, but further studies of this type may reveal whether or not this is a consistent pattern.

References

Arcamone, F. (1978) in *Topics in Antibiotic Chemistry*

(Sammes, P. G., Ed.) pp 95–110, Ellis Horwood, Chichester, U.K.

Arcamone, F. (1981) in *Doxorubicin, Anticancer Antibiotics* (Crooke, S. T., & Reich, S. D., Eds.) Medicinal Chemistry 17, Academic Press, New York.

Arcamone, F. (1984) in *X-ray Crystallography and Drug Action*, pp 367–388, Clarendon Press, Oxford, U.K.

Brown, J. R. (1983) in *Molecular Aspects of Anti-Cancer Drug Action*, pp 57–92, Macmillan Press, London.

Burkhoff, A. M., & Tullius, T. D. (1988) *Nature 331*, 455–457.

Chaires, J. B. (1983) *Biochemistry 22*, 4204–4211.

Chaires, J. B., Fox, K. R., Herrera, J. E., Britt, M., & Waring, M. J. (1987) *Biochemistry 26*, 8227–8236.

Chen, K.-X., Gresh, N., & Pullman, B. (1986) *Mol. Pharmacol. 30*, 279–286.

Coll, M., Aymami, J., van der Marel, G. A., van Boom, J. H., Rich, A., & Wang, A. H.-J. (1989) *Biochemistry 28*, 310–320.

Dickerson, R. E., Bansal, M., Calladine, C. R., Diekmann, S., Hunter, W. N., Kennard, O., von Kitzing, E., Lavery, R., Nelson, H. C. M., Olson, W. K., Saenger, W., Shakked, Z., Sklenar, H., Soumpasis, D. M., Tung, C.-S., Wang, A. H.-J., & Zhurkin, V. B. (1989) *Nucleic Acids Res. 17*, 1797–1803.

Diekmann, S. (1987) *Nucleic Acids Res. 15*, 247–265.

DiMarco, A., Arcamone, F., & Zunino, F. (1974) in *Antibiotics* (Corcoran, J. W., & Hahn, F. E., Eds.) pp 101–128, Springer-Verlag, Berlin.

Drew, H. R., & Dickerson, R. E. (1981) *J. Mol. Biol. 151*, 535–556.

DuVernay, V. H., Patcher, J. A., & Crooke, S. (1979) *Biochemistry 18*, 4024–4029.

Frederick, C. A., Ughetto, G., Ho, P. S., Quigley, G. J., van der Marel, G. A., van Boom, J. H., Wang, A. H.-J., & Rich, A. (1985) in *Abstracts from the Fourth Conversation in Biomolecular Stereodynamics* (Sarma, R. H., Ed.) pp 171–172.

Gessner, R. V., Frederick, C. A., Quigley, G. J., Wang, A. H.-J., & Rich, A. (1989) *J. Biol. Chem. 264*, 7921–7935.

Grimmond, H. E., & Beerman, T. (1982) *Biochem. Pharmacol. 31*, 3379–3386.

Hendrickson, W. A., & Konnert, J. (1981) in *Biomolecular Structure, Conformation, Function and Evolution* (Srinivasan, R., Ed.) pp 43–57, Pergamon Press, Oxford, U.K.

Henry, D. W. (1979) *Cancer Treat. Rep. 63*, 845–854.

Jain, S., Zon, G., & Sundaralingam, M. (1989) *Biochemistry 28*, 2360–2364.

Phillips, D. R., DiMarco, A., & Zunino, F. (1978) *Eur. J. Biochem. 85*, 487–494.

Pigram, W. J., Fuller, W., & Hamilton, L. O. (1972) *Nature, New Biol. 235*, 17–19.

Plumbridge, T. W., & Brown, J. R. (1977) *Biochim. Biophys. Acta 27*, 1881–1886.

Quigley, G. J., Wang, A. H.-J., Ughetto, G., van der Marel, G., van Boom, J. H., & Rich, A. (1980) *Proc. Natl. Acad. Sci. U.S.A. 77*, 7204–7208.

Saenger, W., Hunter, W. N., & Kennard, O. (1986) *Nature 324*, 385–388.

Shakked, Z., Rabinovich, D., Cruse, W. B. T., Egert, E., Kennard, O., Sala, G., Salisbury, S. A., & Viswamitra, M. A. (1981) *Proc. R. Soc. London B 213*, 479–487.

Shakked, Z., Rabinovich, D., Kennard, O., Cruse, W. B. T., Salisbury, S. A., & Viswamitra, M. A. (1983) *J. Mol. Biol. 166*, 183–201.

Ughetto, G. (1988) in *Anthracyclines and Anthracenedione-Based Anti-Cancer Agents* (Lown, J. W., Ed.) pp 5–34, Elsevier, New York.

Ulanovsky, L. E., & Trifonov, E. N. (1987) *Nature 326*, 720–722.

van der Marel, G. A., van Boeckel, C. A. A., Wille, G., & van Boom, J. H. (1981) *Tetrahedron Lett. 22*, 3887–3890.

Wang, A. H.-J. (1987) in *Nucleic Acids and Molecular Biology* (Eckstein, F., & Lilley, D. M. J., Eds.) pp 53–69, Springer-Verlag, Berlin.

Wang, A. H.-J., Quigley, G. J., Kolpak, F. J., Crawford, J. L., van Boom, J. H., van der Marel, G., & Rich, A. (1979) *Nature 282*, 680–686.

Wang, A. H.-J., Ughetto, G., Quigley, G. J., & Rich, A. (1987) *Biochemistry 26*, 1152–1163.

Wing, R., Drew, H., Takano, T., Broka, C., Tanaka, S., Itakura, K., & Dickerson, R. (1980) *Nature 287*, 755–758.

Yoon, C., Privé, G. G., Goodsell, D. S., & Dickerson, R. E. (1988) *Proc. Natl. Acad. Sci. U.S.A. 85*, 6332–6336.

Zunino, F., DiMarco, A., Zaccara, A., & Luoni, G. (1974) *Chem.-Biol. Interact. 9*, 25–35.

Zunino, F., DiMarco, A., Zacarra, A., & Gambetta, R. A. (1980) *Biochim. Biophys. Acta 607*, 206–212.